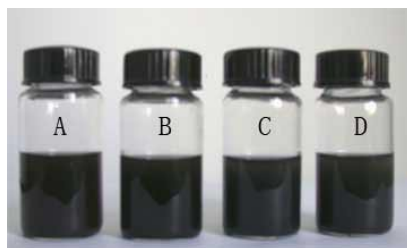


## Supporting Information

1. Figure S1. Photographs of LSMO nanoparticles dispersed in the water. (A)  $x=0$ , (B)  $x=0.3$ , (C)  $x=0.5$ , (D)  $x=0.7$ , respectively.



2. Figure S2-1. EDX data from two parts of individual  $\text{LaMnO}_3$  nanoparticle (a & b) and from other nanoparticles (c).

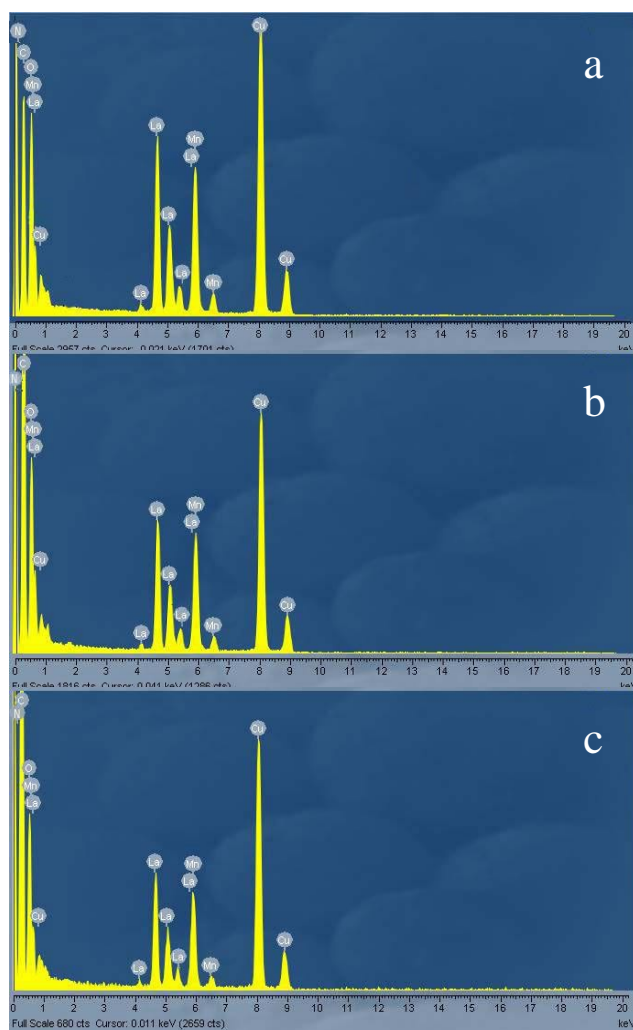


Figure S2-2. EDX data from two parts of an individual  $\text{La}_{0.7}\text{Sr}_{0.3}\text{MnO}_3$  nanoparticle (a & b) and from other nanoparticles (c).

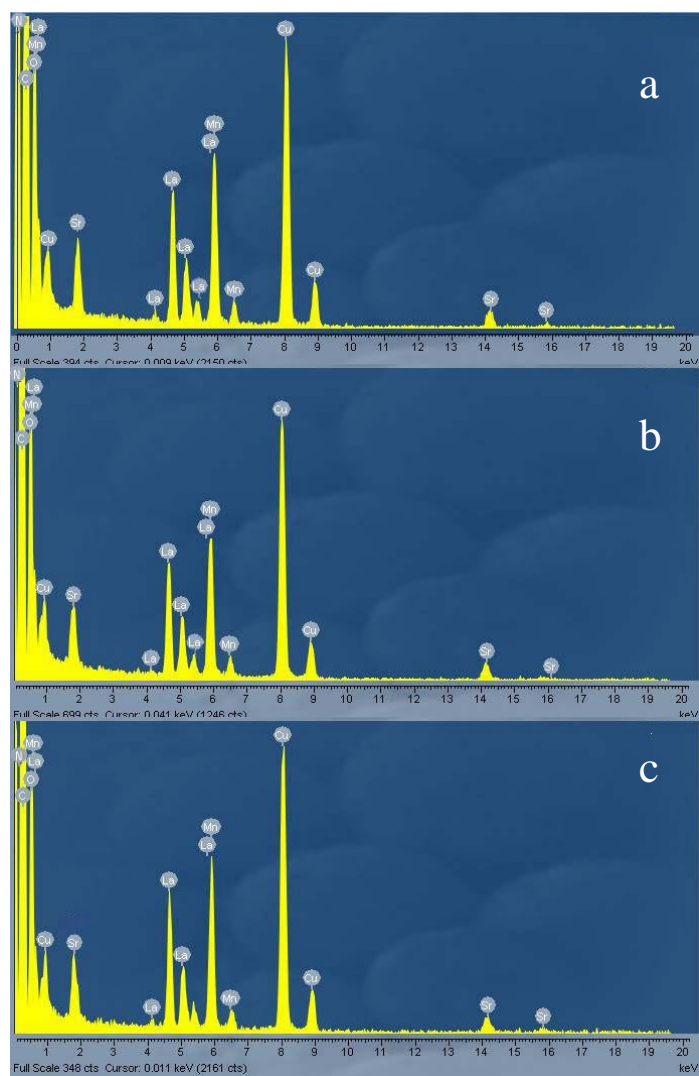


Figure S2-3. EDX data from two parts of an individual  $\text{La}_{0.5}\text{Sr}_{0.5}\text{MnO}_3$  nanoparticle (a & b) and from other nanoparticles (c).

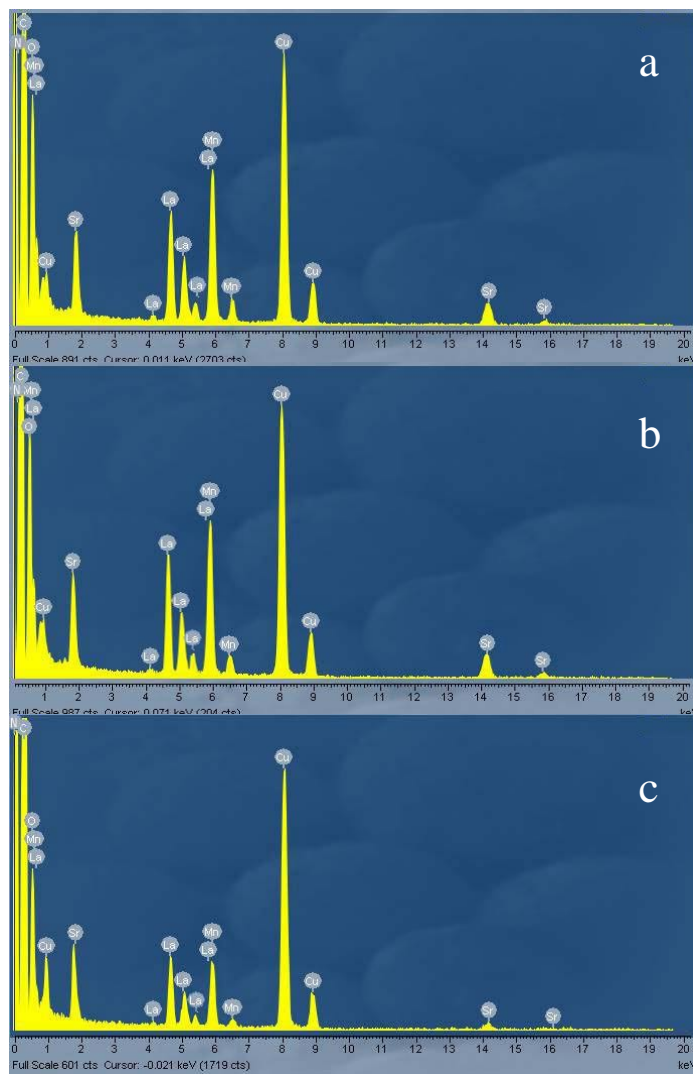
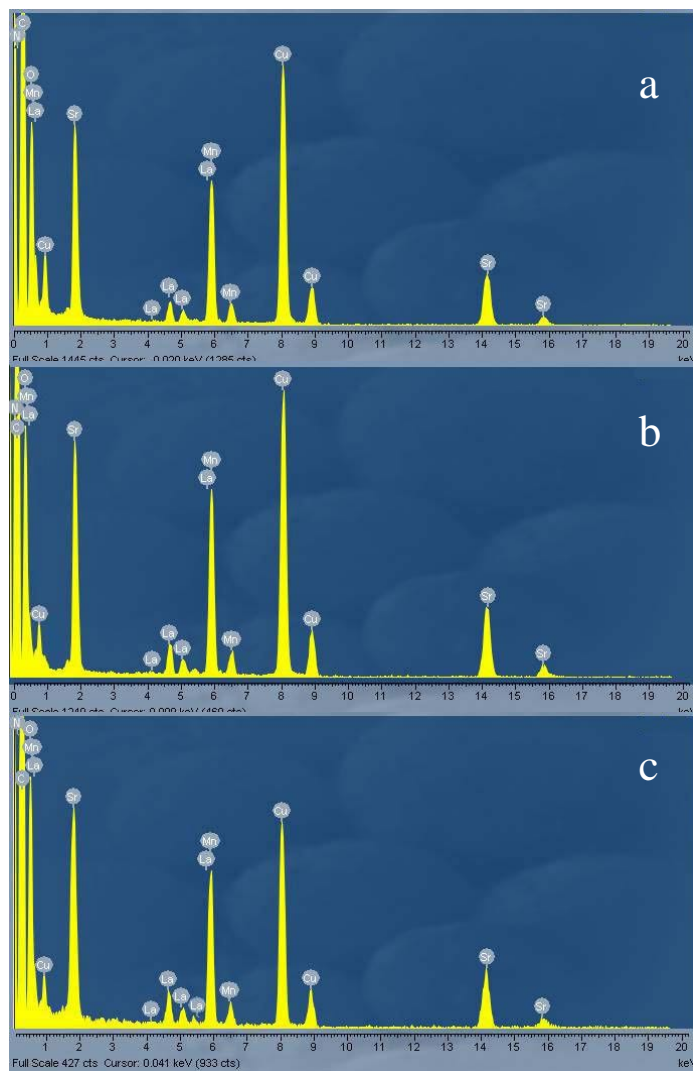
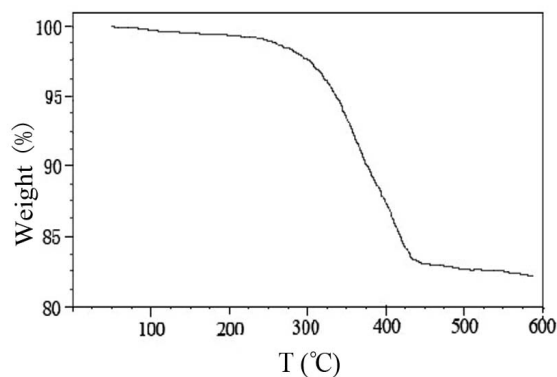


Figure S2-4. EDX data from two parts of an individual  $\text{La}_{0.7}\text{Sr}_{0.3}\text{MnO}_3$  nanoparticle (a & b) and from other nanoparticles (c).



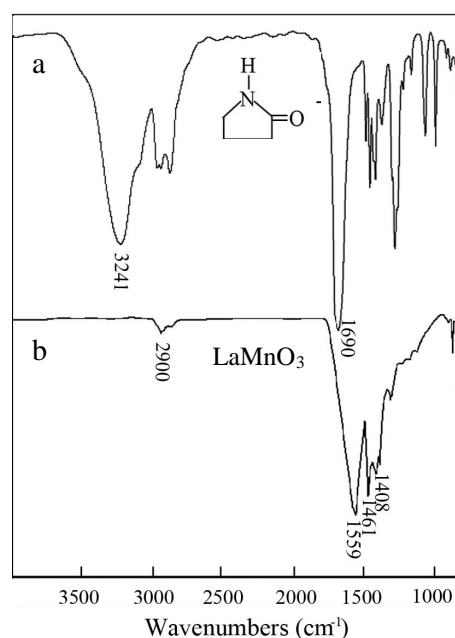
Localized chemical composition analyses by EDX from various parts of individual LSMO nanoparticle and from different particles indicate that all samples exhibit well corrected La, Sr, and Mn elements signals, and stoichiometry as expected within acceptable error limits.

3. Figure S3. Thermal gravimetric (TG) curve of  $\text{LaMnO}_3$  nanoparticles.

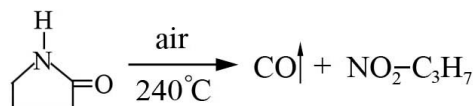


The TG curve of LSMO ( $x=0$ ) nanoparticles shows *ca.*16.9% weight loss from 140 °C to 600 °C (Figure S2), the trivial weight loss ( $\sim 0.38\%$ ) before 140 °C is due to the absorbed water, and the weight loss ( $\sim 0.48\%$ ) after 450 °C might be caused by the fast heating-rate (20 °C/min) and absence of a high-temperature dwell period resulting in the lag of curve. The other samples ( $x=0.3, 0.5, 0.7$ ) contain nearly the same organic content.

4. Figure S4. IR spectra of 2-pyrrolidone (a) and  $\text{LaMnO}_3$  nanoparticles after drying in vacuum (b).

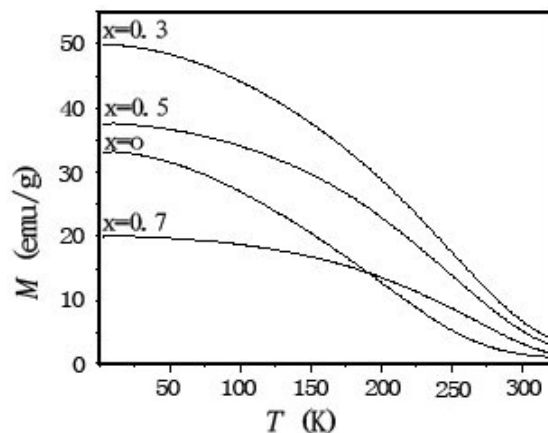


The IR spectrum of 2-pyrrolidone (Figure S4a) shows that the character peaks of amine group ( $3241\text{ cm}^{-1}$ ) and carbonylation group ( $1690\text{ cm}^{-1}$ ). The peaks around  $2900\text{ cm}^{-1}$  are assigned to C-H stretching vibrations, the peaks at  $1461\text{ cm}^{-1}$  and  $1223\text{ cm}^{-1}$  are bending vibrations of C-H, and the peaks at  $1420\text{ cm}^{-1}$  corresponds to C-N stretching vibrations of 2-pyrrolidone. Comparing with the spectrum of 2-pyrrolidone (Figure S4b), the vibrations from the amine group and carbonylation group disappear and the characteristic peak of nitril substitutes them. So the 2-pyrrolidone decomposes into nitril compound during the refluxing process. And the process can be described as:



5. Figure S5. FC curved of four samples. These curves were obtained by cooling each sample to  $T=5\text{ K}$  and then recording  $M$  as the samples were warmed to  $330\text{ K}$  under the application of a magnetic field strong enough to saturate the sample magnetization ( $10\text{ KOe}$ ). The Curie temperatures ( $T_c$ , defined as the maximum of the absolute value of the  $\partial M / \partial T$  derivative) are calculated using the maximum of formula:

$$|f'(x_k)| \approx \left| \frac{f(x_k) - f(x_{k-1})}{x_k - x_{k-1}} \right| = \frac{M(T_{k-1}) - M(T_k)}{T_k - T_{k-1}}.$$



## 6. Experimental Section

To prepare LSMO nanoparticles,  $\text{NaNO}_3$  and  $\text{KNO}_3$  salts were mixed (molar ratio: 2:1) in a nickel crucible and then heated to 550 °C to form a molten salt solvent.  $\text{La}(\text{NO}_3)_3 \cdot 6\text{H}_2\text{O}$ ,  $\text{Mn}(\text{NO}_3)_2 \cdot 4\text{H}_2\text{O}$  and  $\text{Sr}(\text{NO}_3)_2$  depending on the desired molar ratio were mixed and ground in an agate mortar for 10 min, and subsequently put into the molten salt solvent and maintained at 550 °C for 3.0 h. With quick cooling the black solution became solid, it was placed with 2-pyrrolidone in a flask, and then heated at 240 °C until the molten salts dissolved to give a suspension. After cooling to room temperature, the precipitate was separated by centrifugation, washed with ethanol, and dried in a vacuum at 140 °C.

Powder X-ray diffraction (XRD) patterns were collected on a Rigaku D/Max 2200 PC diffractometer with  $\text{CuK}\alpha$  radiation ( $\lambda=1.5418\text{\AA}$ ) and graphite monochromator from 20 to 70° at a scanning rate of 2.0°/min. The particle size, morphology and selected-area electron diffraction (SAED) of the resulting nanoparticles were characterized on a transmission electron microscope (TEM, JEM100-CXII). The structure of nanocrystals was observed by HRTEM (GEOL-2010) equipped with EDX (Oxford). IR (Nicolet 5DX FT-IR instrument, KBr pellet technique), TG (Mettler Toledo, air flow rate 100 mL/min, heating rate 20 °C/min from room temperature to 600 °C) and X-ray photoelectron spectroscopy (XPS) analyses were applied to characterize the nanocrystals' surface. The XPS spectra were recorded on a PHI-5300 ESCA spectrometer (Perkin- Elmer) with its energy analyzer working in the pass energy mode at 35.75 eV, and the  $\text{AlK}\alpha$  line was used as excitation source. The binding energy reference was taken at 284.7 eV for the C1s peak arising from surface hydrocarbons. After subtraction of X-ray satellites and inelastic background (Shirley-type), the peak deconvolution was carried

out. Full width at half maximum (FWHM) was kept the same for chemical components within the same core level of an element, and all component peaks were set to be Gaussian-type. Magnetometry measurements were taken with a Quantum Design PPMS SQUID magnetometer.